Molecular Pharmacology Fast Forward. Published on January 16, 2007 as DOI: 10.1124/mol.106.031161
Molecular Pharmacology Fast Forward. Published on January 16, 2007 as doi:10.1124/mol.106.031161
This article has not been copyedited and formatted. The final version may differ from this version.

Protein Kinase C-Dependent Mitochondrial Translocation of Pro-apoptotic Protein Bax On Activation of Inducible Nitric Oxide Synthase in Rostral Ventrolateral Medulla Mediates Cardiovascular Depression During Experimental Endotoxemia

JULIE Y.H. CHAN, ALICE Y.W. CHANG, LING-LIN WANG,

CHEN-CHUN OU and SAMUEL H.H. CHAN

Department of Medical Education & Research, Kaohsiung Veterans General Hospital,

Kaohsiung 81346 (J.Y.H.C., L.L.W., C.C.O.),

Center for Neuroscience, National Sun Yat-sen University,

Kaohsiung 80424 (A.Y.W.C, S.H.H.C.),

Taiwan, Republic of China.

Downloaded from molpharm.aspetjournals.org at ASPET Journals on April 16, 2024

Copyright 2007 by the American Society for Pharmacology and Experimental Therapeutics.

Molecular Pharmacology Fast Forward. Published on January 16, 2007 as DOI: 10.1124/mol.106.031161
This article has not been copyedited and formatted. The final version may differ from this version.

Bax signaling at RVLM in cardiovascular depression

Address Correspondence to:

Samuel H.H. Chan, PhD,

Center for Neuroscience,

National Sun Yat-sen University,

Kaohsiung 80424, Taiwan, Republic of China.

Tel: +886-7-5255800, Fax: +886-7-5255801,

E-mail: schan@mail.nsysu.edu.tw

Number of text pages: 29

Number of figures: 8

Number of references: 40

Number of words in *Abstract*: 250

Number of words in *Introduction*: 600

Number of words in *Discussion*: 1501

ABBREVIATIONS: aCSF, artificial cerebrospinal fluid; ANT, adenine nucleotide translocase; BA, bongkrekic acid; BCI, 3,6-dibromo-α-(1-piperazinylmethyl)-9H-carbazole-9-ethanol dihydrochloride; carboxyl-PTIO, carboxy-2-phenyl-4,4,5,5-tetramethylimidaxoline-l-oxyl-3-oxide; HR, heart rate; iNOS, inducible nitric oxide synthase; LPS, lipopolysaccharide; mPTP, mitochondrial permeability transition pore; MSAP, mean systemic arterial pressure; P5, Pro-Met-Leu-Lys-Glu; PKC, protein kinase C; RVLM, rostral ventrolateral medulla; SAP, systemic arterial pressure; SMT, S-methylisothiourea; V5, Val-Pro-Met-Leu-Lys; VDAC, voltage-dependent anion protein; z-DEVD-fmk, benzyloxycarbonyl-Val-Ala-Asp (OMe) fluoromethylketone

Downloaded from molpharm.aspetjournals.org at ASPET Journals on April 16, 2024

Molecular Pharmacology Fast Forward. Published on January 16, 2007 as DOI: 10.1124/mol.106.031161
This article has not been copyedited and formatted. The final version may differ from this version.

ABSTRACT

Sympathetic premotor neurons for the maintenance of vasomotor tone are located in rostral ventrolateral medulla (RVLM). We demonstrated previously that overproduction of nitric oxide (NO) by inducible NO synthase (iNOS) in RVLM, leading to caspase 3-dependent apoptotic cell death, plays a pivotal role in cardiovascular depression during endotoxemia induced by intravenous administration of *Escherichia coli* lipopolysaccharide. The interposing intracellular events remain unknown. We evaluated the hypothesis that these events encompass protein kinase C (PKC) activation, which triggers activation and translocation of Bax that opens mitochondrial permeability transition pore by interacting with adenine nucleotide translocase (ANT) or voltage-dependent anion protein (VDAC), followed by cytosolic release of cytochrome *c*. In Sprague-Dawley rats, co-immunoprecipitation and Western blot analyses revealed sequential manifestations during endotoxemia of membrane-bound translocation of PKC, dissociation of cytosolic PKC/Bax complex, mitochondrial translocation of activated Bax, augmented Bax/ANT or Bax/VDAC association, elevated cytosolic cytochrome *c* and caspase 3, and DNA fragmentation in ventrolateral medulla. Microinjection of iNOS inhibitor into bilateral RVLM significantly retarded PKC and Bax activation. The induced association of translocated Bax with ANT or VDAC and the triggered mitochondrial apoptotic signaling cascade were blunted by blockade in RVLM of PKC, mitochondrial translocation of Bax, Bax channels, ANT or caspase 3, alongside significant amelioration of cardiovascular depression. We conclude that formation of mitochondrial Bax/ANT or Bax/VDAC complex that initiates caspase 3-dependent apoptosis in the RVLM as a result of PKC-dependent mitochondrial translocation of activated Bax activated by iNOS-derived NO play a pivotal role in the manifestation of endotoxin-induced cardiovascular depression.

Downloaded from molpharm.aspetjournals.org at ASPET Journals on April 16, 2024

Molecular Pharmacology Fast Forward. Published on January 16, 2007 as DOI: 10.1124/mol.106.031161
This article has not been copyedited and formatted. The final version may differ from this version.

Emerging evidence implicates apoptosis as an important cellular mechanism that underlies the pathogenesis of a variety of cardiovascular disorders, including heart failure (Li et al., 2004), atherosclerosis (Dickhout et al., 2005), ischemia/reperfusion injury (Eefting et al., 2004), and septic shock (Sharahar et al., 2003). Apoptosis is a form of programmed cell death whose initiation and execution are orchestrated by activation of a family of aspartate-specific cysteine proteases called caspases (Takahashi and Earnshaw, 1996). The mitochondrial (caspase 9/caspase 3) pathway, death receptor (caspase 8/caspase 3) pathway and endoplasmic reticulum (caspase 12/caspase 3) pathway represent three distinct routes via which the caspase cascades are activated (Takahashi and Earnshaw, 1996). Of note is that all three pathways converge to caspase 3 activation, leading to DNA fragmentation as the final step to apoptosis.

The rostral ventrolateral medulla (RVLM) is a brain stem site where sympathetic premotor neurons that are responsible for maintaining basal vasomotor tone are located (Ross et al., 1984). We reported previously that, by reducing the sympathetic vasomotor outflow (Chan et al., 2001b), overproduction of nitric oxide (NO) by the inducible NO synthase (iNOS) in the RVLM plays a pivotal role in fatal cardiovascular depression in an animal model of endotoxemia induced by *Escherichia coli* lipopolysaccharide (LPS) (Chan et al., 2001a). We subsequently demonstrated (Chan et al., 2005) that iNOS-derived NO causes the release of cytochrome *c* from the mitochondria to the cytosol, resulting in caspase 3-dependent apoptotic cell death in the RVLM.

The release of apoptosis-initiation factors, including cytochrome *c*, from the intermediate space via mitochondrial permeability transition pore (mPTP) (Martinou and Green, 2001) plays a key role in the subsequent apoptosome formation and caspase 3 activation (Liu et al., 1996). Composed of adenine nucleotide translocase (ANT) and voltage-dependent anion protein (VDAC) (Halestrap and Brennerb, 2003), opening of the mPTP is reciprocally regulated by various Bcl-2 family proteins. Thus, anti-apoptotic proteins such as Bcl-2 and Bcl-xL reduce, and pro-apoptotic proteins

Downloaded from molpharm.aspetjournals.org at ASPET Journals on April 16, 2024

Molecular Pharmacology Fast Forward. Published on January 16, 2007 as DOI: 10.1124/mol.106.031161
This article has not been copyedited and formatted. The final version may differ from this version.

such as Bax and Bak enhance mitochondrial cytochrome *c* release (Kroemer, 1997). On activation of death signals, Bax translocates from the cytosol to the mitochondria and increases mitochondrial membrane permeabilization via interactions with ANT and/or VDAC (Shimizu et al., 1999). As such, Bax may serve as an intracellular trigger for mitochondrion-dependent apoptosis.

We identified recently (Chang et al., 2006) an interplay between Bax and caspase 3-dependent apoptotic cell death in the RVLM during experimental endotoxemia. The intracellular signals that interpose between generation of NO, activation and translocation of Bax, and cytosolic release of cytochrome *c* in this apoptotic cascade are unknown. One potential candidate is protein kinase C (PKC). LPS mediates its cellular effects via Toll-like receptor 4-associated second messenger pathways, including PKC (Comalada et al., 2003), and mitochondrial translocation of activated Bax following its dissociation from the PKC/Bax complex is engaged in hypoxia/reperfusion-induced apoptosis in endothelial cell (Wang et al., 2005). We hypothesize that generation of NO by upregulation of iNOS in the RVLM leads to PKC activation, which triggers activation and translocation of Bax that opens mPTP by interacting with ANT or VDAC in the mitochondria, followed by activation of the cytochrome *c*-caspase 3 apoptotic cascade, underlie cardiovascular depression during endotoxemia. The present study validated this hypothesis. We demonstrated that iNOS activation in the RVLM after LPS treatment resulted in membrane bound translocation of PKC from the cytosol and the dissociation of PKC/Bax complex. Following mitochondrial translocation, the activated Bax formed a heterodimeric complex with ANT and VDAC, leading to cytochrome *c* release, activation of caspase 3 and DNA fragmentation in the RVLM. Most importantly, these cellular events play a crucial role in the manifestation of endotoxin-induced cardiovascular depression.

Downloaded from molpharm.aspetjournals.org at ASPET Journals on April 16, 2024

Molecular Pharmacology Fast Forward. Published on January 16, 2007 as DOI: 10.1124/mol.106.031161
This article has not been copyedited and formatted. The final version may differ from this version.

Materials and Methods

All experimental procedures were carried out in compliance with the guidelines of our institutional animal care committee, and were in accordance with the Guide for the Care and Use of Laboratory Animals as adopted and promulgated by the U.S. National Institutes of Health.

Animals. Experiments were carried out in adult male Sprague-Dawley rats (200 to 270 g, n = 268) purchased from the Experimental Animal Center of the National Applied Research Laboratories, Taiwan. They were housed in an animal room under temperature control (24 ± 0.5°C) and 12-h light-dark (08:00-20:00) cycle. Standard laboratory rat chow (PMI Nutrition International, Brentwood, MO) and tap water were available *ad libitum*. All animals were allowed to acclimatize for at least 7 days prior to experimental manipulations.

General Preparation. Rats were anesthetized initially with pentobarbital sodium (50 mg/kg, ip) to perform preparatory surgery (Chan et al., 2001a,b, 2002, 2005), which routinely included intubation of the trachea and cannulation of the femoral artery and vein. Animals received thereafter continuous intravenous infusion of propofol (30 mg/kg/h), which provided satisfactory anesthetic maintenance while preserving the capacity of central cardiovascular regulation (Yang et al., 1995). Animals were mechanically ventilated to maintain end-tidal CO_2 to be within 4 to 5%, as monitored by a capnograph (Datex Normocap, Helsinki, Finland). All data were collected from animals with a maintained rectal temperature of 37 ± 0.5°C. At the end of each experiment, rats were killed with intravenous injection of an over-dose of pentobarbital sodium (100 mg/kg).

Power Spectral Analysis of SAP Signals. Pulsatile and mean systemic arterial pressure (MSAP), as well as heart rate (HR), were recorded on a polygraph (Gould,

Downloaded from molpharm.aspetjournals.org at ASPET Journals on April 16, 2024

Molecular Pharmacology Fast Forward. Published on January 16, 2007 as DOI: 10.1124/mol.106.031161
This article has not been copyedited and formatted. The final version may differ from this version.

Valley View, OH), along with simultaneous on-line and real-time power spectral analysis of the SAP signals (Chan et al., 2001a,b, 2002). We were particularly interested in the very low-frequency (0-0.25 Hz) and low-frequency (0.25-0.8 Hz) components in the SAP spectrum. Our laboratory demonstrated previously (Kuo et al., 1997) that these spectral components of SAP signals take origin from the RVLM, and their power density reflects the prevailing neurogenic sympathetic vasomotor tone.

Induction of Experimental Endotoxemia. Experimental endotoxemia was induced by intravenous injection of *Escherichia coli* lipopolysaccharide (LPS, 15 mg/kg, serotype 0111:B4; Sigma-Aldrich, St. Louis, MO) (Chan et al., 2001a, 2005; Chang et al., 2006). Injection of the same amount of 0.9% saline served as the vehicle and volume control. The temporal changes in mean SAP, HR and power density of the vasomotor components of the SAP signals were routinely followed for 6 h.

Microinjection of Test Agents into the RVLM. Test agents were microinjected bilaterally and sequentially, at a volume of 50 nl, into the RVLM (Chan et al., 2001a,b, 2002, 2005; Chang et al., 2006). The coordinates for RVLM were 4.5-5 mm posterior to lambda, 1.8-2.1 mm lateral to the midline, and 8.0-8.5 mm below the dorsal surface of cerebellum. Test agents used included an iNOS inhibitor, S-methylisothiourea (SMT; Tocris Cookson, Bristol, UK); a NO trapping agent, carboxy-2-phenyl-4,4,5,5-tetramethylimidaxoline-l-oxyl-3-oxide (carboxy-PTIO, Tocris Cookson); selective PKC inhibitors, calphostin C or Gö6983 (Calbiochem, San Diego, CA); a chloride channel inhibitor that blocks mitochondrial translocation of Bax, furosemide (Sigma-Aldrich); cell membrane-permeable Bax inhibitor peptides, Pro-Met-Leu-Lys-Glu (P5; Tocris Cookson) or Val-Pro-Met-Leu-Lys (V5; Tocris Cookson); a Bax channel inhibitor (BCI), 3,6-dibromo-α-(1-piperazinylmethyl)-9H-carbazole-9-ethanol dihydrochloride (Tocris Cookson); an inhibitory ligand of the mitochondrial ANT, bongkrekic acid (BA; Sigma-Aldrich); or a cell-permeable caspase 3 inhibitor,

Downloaded from molpharm.aspetjournals.org at ASPET Journals on April 16, 2024

Molecular Pharmacology Fast Forward. Published on January 16, 2007 as DOI: 10.1124/mol.106.031161
This article has not been copyedited and formatted. The final version may differ from this version.

benzyloxycarbonyl-Val-Ala-Asp (OMe) fluoromethylketone (z-DEVD-fmk; Calbiochem). The dose and treatment scheme were adopted from previous reports (Chan et al., 2001b, 2005; Wu et al., 2003) that used the same test agents for the same purpose as in this study or established during the initial pilot studies. With the exception of Gö6983, BCI or z-DEVD-fmk, which used 1% DMSO as the solvent, all test agents were prepared with artificial cerebrospinal fluid (aCSF). Microinjection of these two solvents served as the vehicle and volume control.

Collection of Ventrolateral Medullary Samples. Rats were killed with an overdose of pentobarbital sodium and perfused intracardiacally with 150 ml of warm (37°C) saline containing heparin (100 U/ml). The brain was rapidly removed and placed on dry ice. Both sides of the ventrolateral medulla, at the level of the RVLM (0.5 to 1.5 mm rostral to the obex), were collected by micropunches made with a stainless steel bore (1 mm, id). Medullary tissues collected from animals under anesthesia but without treatment served as the sham control.

Isolation of Membranous, Cytosolic or Mitochondrial Fractions. We isolated membranous, cytosolic or mitochondrial fraction by discontinuous Percoll gradient centrifugation according to procedures described previously (Chuang et al., 2002; Chan et al., 2005). This procedure yields 10-15% of the total mitochondria, and enriches the mitochondrial fraction by at least 10-fold when compared with tissue homogenates (Kantrow et al., 1997). The amount of protein in each fraction was determined by the method of Bradford with a protein assay kit (Bio-Rad, Hercules, CA).

Western Blot Analysis. Western blot analysis (Chan et al., 2002, 2005; Chang et al., 2006) was carried out on proteins extracted from the membranous, cytosolic or mitochondrial fraction. The primary antiserum used in this study included rabbit polyclonal anti-PKC (1:1000; Calbiochem), anti-PKC-α (1:500; Calbiochem),

Downloaded from molpharm.aspetjournals.org at ASPET Journals on April 16, 2024

Molecular Pharmacology Fast Forward. Published on January 16, 2007 as DOI: 10.1124/mol.106.031161
This article has not been copyedited and formatted. The final version may differ from this version.

anti-PKC-βI (1:2000; Calbiochem), anti-PKC-βII (1:2000; Calbiochem), anti- PKC-γ (1:2000; Calbiochem), anti-PKC-δ (1:2000; Calbiochem), anti-PKC-ε (1:1000; Calbiochem), anti-PKC-η (1:1000; Calbiochem), anti-PKC-ζ (1:2000; Calbiochem), anti-PKC-ι (1:2000; Calbiochem), anti-cytochrome *c* (1:1000 and 1:5000 for cytosolic and mitochondrial fractions; Oncogene), anti-caspase 3 that recognizes the inactive pro-caspase 3 (36 KDa) and the active cleaved fragment (20 KDa) of caspase 3 (1:1000; Calbiochem), anti-Bcl-xL (1:1000; Calbiochem), anti-Bcl-2 (1:1000; Calbiochem), anti-ANT (1:1000; Santa Cruz Biotechnology, Santa Cruz, CA), anti-VDAC (1:1000; Santa Cruz Biotechnology), anti-HSP70 (1:2000; Stressgen, Victoria, Canada) or anti-α-tubulin (1:5000; Sigma-Aldrich) antiserum. The secondary antisera used included horseradish peroxidase-conjugated anti-rabbit or anti-mouse IgG (1:5000; Jackson Immunoresearch Laboratories, West Grove, PA). Specific antibody-antigen complex was detected by an enhanced chemiluminescence Western blot detection system (PerkinElmer Life Sciences, Boston, MA). The amount of protein was quantified by Photo-Print Plus software (ETS Vilber-Lourmat, France), and was expressed as the ratio (%) to α-tubulin protein, which served as the internal control to demonstrate equal loading of the proteins.

Immunoprecipitation. For immunoprecipitation assay (Chang et al., 2006), protein A- or G-agarose beads were added to each protein fraction. Immunoprecipitation with either a mouse monoclonal anti-Bax 6A7 antiserum that recognizes specifically the conformational change in Bax protein associated with its activation (Yethon et al., 2003) or a rabbit polyclonal anti-Bcl-2, anti-Bcl-xL, anti-ANT, anti-VDAC or anti-PKC antiseum was performed at 4°C overnight and the precipitated beads were washed with an ice-cold lysis buffer followed by a kinase buffer (25 mM HEPES, pH 7.4, 20 mM $MgCl_2$, 0.1 mM Na_3VO_4, 2 mM dithiothreitol). Western blot analysis of Bax (1:1000; Calbiochem) was carried out as described above.

Downloaded from molpharm.aspetjournals.org at ASPET Journals on April 16, 2024

Molecular Pharmacology Fast Forward. Published on January 16, 2007 as DOI: 10.1124/mol.106.031161
This article has not been copyedited and formatted. The final version may differ from this version.

Sandwich ELISA for Histone-Associated DNA Fragmentation. To quantify apoptosis-related DNA fragmentation, a cell death enzyme-linked immunosorbent assay (Roche Molecular Biochemicals, Mannheim, Germany) that detects apoptotic but not necrotic cell death (Bonfoco et al., 1995) was used to assay the level of histone-associated DNA fragments in the cytoplasm (Saito et al., 2004). In brief, protein from the cytosolic fraction of the ventrolateral medullary samples was used as the antigen source, together with primary anti-histone antibody and secondary anti-DNA antibody coupled to peroxidase. The amount of nucleosomes in cytoplasm was quantitatively determined using 2,2'-azino-di-[3-ethylbenzthiazoline sulfonate] as the substrate. Absorbance was measured at 405 nm and referenced at 490 nm using a microtiter plate reader (Hitachi, Japan).

Histology. For verification of microinjection sites, the brain stem, except those dissected by micropunches for extraction of protein, was removed from animals after the physiological experiments and fixed in 30% sucrose in 10% formaldehyde-saline solution for ≥ 72 h. Frozen 25-μm sections of the medulla oblongata were stained with 1% Neural red for histological verification of the location of microinjection sites. One percent Evans blue was added to the microinjection solution to facilitate this process.

Statistical Analysis. All values are expressed as mean ± SE. One-way or two-way analysis of variance with repeated measures was used to assess group means, as appropriate, to be followed by the Scheffé multiple-range test for post hoc assessment of individual means. $p < 0.05$ was considered statistically significant.

Downloaded from molpharm.aspetjournals.org at ASPET Journals on April 16, 2024

Molecular Pharmacology Fast Forward. Published on January 16, 2007 as DOI: 10.1124/mol.106.031161
This article has not been copyedited and formatted. The final version may differ from this version.

Results

Differential Activation of PKC Isoforms in Ventrolateral Medulla During Experimental Endotoxemia. Our first series of experiments determined the extent of PKC isoform activation in the RVLM after LPS treatment (15 mg/kg, iv), using membrane bound translocation of PKC from the cytosol as our experimental index (Buchner et al., 1999). Western blot analysis revealed an increased expression of PKC-βI, PKC-γ, PKC-δ or PKC-ζ isoform in the membranous fraction of samples from ventrolateral medulla during experimental endotoxemia, accompanied by a concomitant decrease of those PKC isoforms in the cytosolic fraction (Fig. 1). This membrane translocation of PKC-βI, PKC-γ, PKC-δ or PKC-ζ occurred 15 min after LPS administration, lasting at least 60 min. The expression of PKC-α or PKC-ε isoforms in the cytosolic or membranous fraction, on the other hand, remained unchanged. In addition, expression of PKC-βII, PKC-η or PKC-ι in both fractions was below our detection limit (data not shown).

Inducible NOS-Dependent Activation of PKC Isoforms in Ventrolateral Medulla During Experimental Endotoxemia. We next ascertained a causal involvement of iNOS-derived NO in the activation of PKC isoforms at the RVLM. Compared to aCSF, microinjection bilaterally into the RVLM of the iNOS inhibitor, SMT (250 pmol) immediately following LPS administration significantly antagonized the induced upregulation of PKC-βI, PKC-γ, PKC-δ or PKC-ζ expression in the membranous fraction of samples from ventrolateral medulla (Fig. 2). Similar observations were found in animals that received the NO trapping agent, carboxy-PTIO (50 nmol) in the bilateral RVLM (data not shown). SMT or carboxy-PTIO, on the other hand, had no effect on basal cytosolic or membranous expression of those PKC isoforms (data not shown).

Downloaded from molpharm.aspetjournals.org at ASPET Journals on April 16, 2024

Molecular Pharmacology Fast Forward. Published on January 16, 2007 as DOI: 10.1124/mol.106.031161
This article has not been copyedited and formatted. The final version may differ from this version.

Inducible NOS-Dependent Dissociation of PKC From Bax in Ventrolateral Medulla During Experimental Endotoxemia. Our third series of experiments evaluated the degree of association between PKC and Bax in the cytosolic fraction of medullary samples under resting condition or during experimental endotoxemia. Immunoprecipitation coupled with immunoblot revealed that PKC in ventrolateral medulla was associated with Bax under basal condition (Fig. 3A). The extent of this association underwent a gradual reduction that became discernibly different from baseline 120 or 240 min after LPS treatment. Such a dissociation of the PKC/Bax complex was blunted in the presence of SMT (250 pmol). As a control, the amount of precipitated Bax remained constant throughout this series of experiments.

Mitochondrial Translocation of Activated Bax in Ventrolateral Medulla During Experimental Endotoxemia. We next investigated whether mitochondrial translocation of activated Bax from the cytosol took place in the RVLM during experimental endotoxemia. Co-immunoprecipitation experiments pairing an anti-6A7 antiserum that specifically recognizes the conformational change in Bax protein associated with its activation with an anti-Bax antiserum or vice versa (Fig. 3B) also revealed a progressive increase in the expression of activated Bax in ventrolateral medulla, measured 60, 120 or 240 min after LPS administration. Whereas SMT treatment (250 pmol) again suppressed this endotoxin-promoted Bax activation, the total Bax expression in ventrolateral medulla was unaffected by LPS, given alone or with SMT. We further demonstrated in samples obtained from ventrolateral medulla 120 min after LPS treatment that the appreciable increase in activated Bax was present in both the cytosolic and mitochondrial fraction (Figs. 3C and 3D). Whereas this augmentation of cytosolic and mitochondrial Bax was blunted by the PKC inhibitors, calphostin C (100 pmol) or Gö6983 (100 pmol) (Fig. 3C), only the increase in mitochondrial Bax was attenuated by inhibition of Bax translocation with furosemide (1, 5 or 10 nmol) (Fig. 3D). Furosemide, at the same time, caused further increases in activated Bax expression in the cytosol (Fig. 3D).

Downloaded from molpharm.aspetjournals.org at ASPET Journals on April 16, 2024

Molecular Pharmacology Fast Forward. Published on January 16, 2007 as DOI: 10.1124/mol.106.031161
This article has not been copyedited and formatted. The final version may differ from this version.

Association of Activated Bax with Mitochondrial ANT or VDAC in Ventrolateral Medulla During Experimental Endotoxemia. Our fifth series of experiments determined the mitochondrial target of the activated Bax during experimental endotoxemia. Whereas complex formation between activated Bax and ANT or VDAC was below detection limit under basal condition (Fig. 4A), samples collected from ventrolateral medulla 60, 120 or 240 min after LPS treatment revealed a progressive increase in the association between ANT or VDAC and activated Bax in the mitochondrial fraction. Intriguingly, this mitochondrial Bax/ANT or Bax/VDAC immunocomplex was appreciably reduced in the presence of furosemide (10 nmol) (Fig. 4A), the Bax channel inhibitor, BCI (0.5 nmol) or the ANT inhibitor, BA (1 μmol) (Fig. 4B). As a control, the increased Bax/ANT or Bax/VDAC heterodimerization was not accompanied by changes in ANT or VDAC protein expression in the mitochondrial fraction of samples from ventrolateral medulla. At the same time, formation of the Bax/Bcl-2 or Bax/Bcl-xL complex was below detection limit throughout this series of experiments (Fig. 4A).

Bax-Dependent Release of Mitochondrial Cytochrome *c*, Activation of Caspase 3 or DNA Fragmentation in Ventrolateral Medulla During Experimental Endotoxemia. Similar to our previous observations (Chan et al., 2005; Chang et al., 2006), experimental endotoxemia was accompanied by the release of cytochrome *c* from the mitochondria to the cytosol, followed by activation of the pro-apoptotic caspase 3 in ventrolateral medulla (Fig. 5A). Upregulation of cytosolic cytochrome *c* was detected 120 min, and activated caspase 3 was expressed 180 min after LPS treatment. Microinjection bilaterally into the RVLM of BCI (0.5 nmol) (Fig. 5A) or BA (1 μmol) (data not shown) significantly antagonized this LPS-induced cytochrome *c* release or caspase 3 activation. The same treatments, along with furosemide (10 nmol) or the caspase 3 inhibitor, z-DEVD-fmk (100 nmol), also significantly suppressed DNA fragmentation induced in ventrolateral medulla during experimental

Downloaded from molpharm.aspetjournals.org at ASPET Journals on April 16, 2024

Molecular Pharmacology Fast Forward. Published on January 16, 2007 as DOI: 10.1124/mol.106.031161
This article has not been copyedited and formatted. The final version may differ from this version.

endotoxemia (Fig. 5B).

Causal Involvement of PKC, Bax, ANT or Caspase 3 at RVLM in Cardiovascular Depression During Experimental Endotoxemia. As reported previously by our laboratory (Chan et al., 2001a, Chang et al., 2006), LPS treatment resulted in an initial, followed by a delayed decline in MSAP and HR, along with a reduction in the power density of the vasomotor components of SAP signals during the 360-min observation period (Figs. 6 and 7). Compared with vehicle controls, microinjection immediately after LPS administration into the bilateral RVLM of calphostin C (50 or 100 pmol) (Figs. 6A and 8A); furosemide (5 or 10 nmol) (Fig. 8A); Bax inhibitor peptides, V5 (10 or 20 pmol) or P5 (10 or 20 pmol) (Fig. 8A); BCI (0.5 or 1 nmol) (Figs. 7A and 8A); BA (5 or 10 nmol) (Fig. 8A); or z-DEVD-fmk, (50 or 100 nmol) (Fig. 8A), significantly antagonized the cardiovascular depression during experimental endotoxemia. Of note is that, given 120 min after LPS treatment, furosemide (Fig. 8B), V5 or P5 (Fig. 8B), BCI (Figs. 7B and 8B), BA (Fig. 8B) or z-DEVD-fmk (Fig. 8B), but not calphostin C (Figs. 6B or 8B), significantly attenuated the LPS-promoted decrease in MSAP, HR or sympathetic neurogenic vasomotor tone.

Histology. Based on the location of the tip of the microinjection needle, histological verifications indicated that our results were obtained from animals that received local application of the test agents or vehicle within the confines of the RVLM. Microinjection of test agents to sites adjacent to the RVLM was ineffective.

Discussion

We reported recently (Chan et al., 2005) that iNOS-derived NO triggers the cytosolic release of mitochondrial cytochrome *c* during experimental endotoxemia,

Downloaded from molpharm.aspetjournals.org at ASPET Journals on April 16, 2024

Molecular Pharmacology Fast Forward. Published on January 16, 2007 as DOI: 10.1124/mol.106.031161
This article has not been copyedited and formatted. The final version may differ from this version.

resulting in caspase 3-dependent apoptotic cell death in the RVLM. We further showed (Chang et al., 2006) that this process involves the participation of the pro-apoptotic protein Bax. The present study provided the novel identification that activated PKC represents the crucial interposing intracellular signal that triggers mitochondrial translocation of Bax after iNOS activation. Specifically, we demonstrated that the temporal sequence of signaling events following activation of iNOS in the RVLM during experimental endotoxemia includes membrane bound translocation of cytosolic PKC, dissociation of the cytosolic PKC/Bax complex, mitochondrial translocation of Bax, heterodimerization between activated Bax and ANT or VDAC, cytosolic release of cytochrome *c*, activation of caspase 3 and DNA fragmentation. Most importantly, we demonstrated that formation of mitochondrial Bax/ANT or Bax/VDAC complex that initiates apoptosis in the RVLM as a result of PKC-dependent mitochondrial translocation of activated Bax plays a pivotal role in the manifestation of endotoxin-induced cardiovascular depression.

Membrane bound translocation of PKC from the cytosol is a hallmark of PKC activation (Buchner et al., 1999). Accordingly, the present study revealed an early activation of conventional PKCβI or γ, novel PKCδ, and atypical PKCζ isoforms in ventrolateral medulla after LPS treatment. Ischemia/reperfusion injury results in activation of PKCδ in the hippocampus (Bright and Mochly-Rosen, 2005), and an early activation of PKCζ is involved in the NMDA-induced apoptosis in cortical neurons (Crisanti et al., 2005). The reversal by SMT of membrane bound translocation of all those PKC isoforms further supports a causal relationship between the iNOS-derived NO and PKC activation. NO may activate PKC via at least two mechanisms. One is by reacting with superoxide anion to form peroxynitrite that activates PKC (Lochner et al., 2000), and the other is by direct nitration of tyrosine residues in PKC (Balafanova et al., 2002). It is therefore of interest that we reported previously (Chan et al., 2002) that formation of peroxynitrite by a reaction between iNOS-derived NO and superoxide anion in the RVLM contributes primarily to cardiovascular depression during experimental endotoxemia.

Downloaded from molpharm.aspetjournals.org at ASPET Journals on April 16, 2024

Molecular Pharmacology Fast Forward. Published on January 16, 2007 as DOI: 10.1124/mol.106.031161
This article has not been copyedited and formatted. The final version may differ from this version.

Our data showed that PKC forms a complex with Bax under basal condition in ventrolateral medulla. Intriguingly, PKC activation on LPS treatment was accompanied by the dissociation of this PKC/Bax complex, concurrent with elevated levels of activated Bax that was inhibited by SMT or PKC inhibitors. These results suggest, for the first time, that membrane bound translocation of PKC after iNOS activation leads to dissociation of PKC from the complex, which triggers conformational changes that transform Bax to an active form that in turn translocates to the mitochondria. Of note is that activation and translocation of Bax, which was readily detectable in the mitochondrial fraction 60 min after LPS treatment, occurred without a decrease in overall Bax expression in the cytosol. This observation suggests that de novo synthesis of Bax may contribute to the increase in Bax translocation during endotoxemia. A conformational change in Bax as a result of changes in the ionic composition of the cytosolic milieu underlies intracellular translocation of Bax (Roucou and Martinou, 2001). It is therefore intriguing to note that furosemide dose-relatedly reduced the augmented expression of the activated Bax in the mitochondria, alongside further increases in cytosolic Bax expression. These results are interpreted to suggest that by inhibiting the chloride channels, furosemide may alter the cytosolic pH and/or ionic strength (Cooper and Hunter, 1997) and effectively prevent the conformational change in Bax that is required for mitochondrial translocation.

Conflicting reports exist on whether PKC inhibits apoptosis (Pierchala et al., 2004; Weinreb et al., 2004), or mediates apoptotic processes (Bright et al., 2004; Bright and Mochly-Rosen, 2005). Bax moves from the cytosol to mitochondria under conditions that induce cell death by apoptosis (Wolter et al., 1997). The present study provided novel demonstration that a key determinant of this Bax-dependent apoptotic activity in the RVLM during experimental endotoxemia is the extent of association between PKC and Bax. We further observed that the temporal profile of Bax translocation to the mitochondria after LPS treatment coincided with that of cytochrome *c* release to the cytosol, and was followed by activation of caspase 3 and apoptotic cell death in

Downloaded from molpharm.aspetjournals.org at ASPET Journals on April 16, 2024

Molecular Pharmacology Fast Forward. Published on January 16, 2007 as DOI: 10.1124/mol.106.031161
This article has not been copyedited and formatted. The final version may differ from this version.

ventrolateral medulla. More importantly, that furosemide prevented all those LPS-induced apoptotic signalling indicated that mitochondrial translocation of Bax on dissociation from the activated PKC is a prerequisite for triggering the cytochrome *c*-caspase 3 cascade of mitochondrial apoptotic event in the RVLM during endotoxemia.

The importance of Bax in the execution of mitochondrial death pathway was reported in a recent study in which denervation-induced cytochrome *c* release, increase in caspase 3 activity and apoptotic cell death in the muscle are absent in Bax-knockout mice (Siu and Always, 2006). There are two mechanisms by which Bax may target mitochondria to trigger apoptotic cell death (Adams and Cory, 1998). One is for Bax to interact with anti-apoptotic members of Bcl-2 family such as Bcl-2 and Bcl-xL to block their actions, and the other is to directly enhance the mitochondrial outer membrane permeability. The present study provided novel demonstration that enhanced Bax/ANT or Bax/VDAC interactions in mitochondria, but not association of Bax with Bcl-2 or Bcl-xL, contributes to the LPS-promoted apoptotic cell death in the RVLM during experimental endotoxemia. Heterodimerization between Bax and ANT or VDAC directly changes the conformation of mPTP and increases membrane permeability (Shimizu et al., 1999; Cao et al., 2001), and the release of cytochrome *c* from mPTP plays a key role in triggering caspase 3 activation and the associated mitochondrial apoptotic pathway (Liu et al., 1996; Halestrap and Brennerb, 2003). Furthermore, ectopic expression of Bax-induced apoptosis occurs in wild-type but not in ANT- or VDAC-deficient cells (Shimizu et al., 1999). Our observations that Bax channel or ANT inhibitor significantly reduced the formation of Bax/ANT or Bax/VDAC complex, suppressed release of cytochrome *c* into the cytosol and attenuated LPS-induced apoptosis in the RVLM are therefore consistent with the stipulated enhancement of mitochondrial outer membrane permeability by Bax in the initiation of the apoptotic pathway. A reduction in LPS-promoted formation of mitochondrial Bax/ANT or Bax/VDAC complex in the presence of furosemide further suggests that only activated Bax that translocates to the mitochondria is associated

Downloaded from molpharm.aspetjournals.org at ASPET Journals on April 16, 2024

Molecular Pharmacology Fast Forward. Published on January 16, 2007 as DOI: 10.1124/mol.106.031161
This article has not been copyedited and formatted. The final version may differ from this version.

with this complex.

NO derived from iNOS in the RVLM suppresses sympathetic neurogenic vasomotor activity and induces severe hypotension and bradycardia after LPS treatment (Chan et al., 2001a; 2002). Perhaps the most intriguing finding of the present study is the demonstration, for the first time, that our identified PKC-dependent mitochondrial translocation of activated Bax, formation of mitochondrial Bax/ANT and Bax/VDAC complexes, cytosolic release of cytochrome *c* and caspase 3-dependent apoptosis in the RVLM represent a crucial cascade of intracellular events that are triggered by iNOS-derived NO, and plays a pivotal role in the manifestation of cardiovascular depression during endotoxemia. That treatments with the same PKC, Bax translocation or Bax channel inhibitors at doses that sufficiently blunted the relevant cellular events also significantly attenuated the LPS-promoted decrease in MSAP, HR or sympathetic neurogenic vasomotor tone provided ample support for this notion. We noted that whereas pharmacological blockade of mitochondrial Bax translocation or Bax-associated mitochondrial apoptotic signaling delivered 120 min after LPS treatment was effective against the late stage cardiovascular depression, co-administration of PKC inhibitors into the RVLM at this time point exerted minimal effects. These observations are again complementary to our biochemical results and reinforced the contention that iNOS-dependent activation of PKC constitutes an early step of cellular events that mediate LPS-induced cardiovascular depression. The contribution of PKCβI, PKCγ, PKCδ or PKCζ isoforms to apoptosis in the RVLM and cardiovascular depression during experimental endotoxemia, however, requires further delineation.

Human and animal studies have shown that cardiovascular depression is a crucial and often fatal event that may lead to multiple organ failure during endotoxemia. Whereas endotoxemia is a well-defined clinical phenomenon, the pathogenic basis and the molecular mediators that trigger circulatory depression, particularly in brain areas that are involved in cardiovascular regulation, remain poorly understood. Based on results from the present study, we propose that iNOS-derived NO triggered during

Downloaded from molpharm.aspetjournals.org at ASPET Journals on April 16, 2024

Molecular Pharmacology Fast Forward. Published on January 16, 2007 as DOI: 10.1124/mol.106.031161
This article has not been copyedited and formatted. The final version may differ from this version.

endotoxemia induces membrane bound translocation of PKC, resulting in dissociation of cytosolic PKC/Bax complex, to be followed by mitochondrial translocation of the activated Bax, formation of mitochondrial Bax/ANT or Bax/VDAC complex, leading to cytosolic release of cytochrome *c* and execution of caspase 3-associated apoptotic cell death in the RVLM. Most importantly, this cascade of intracellular events plays a pivotal role in the elicitation of cardiovascular depression during endotoxemia. This detailed dissection of the intracellular signaling mechanisms in the RVLM after iNOS activation opens a new therapeutic vista in our search for new and more effective agents against cardiovascular depression during endotoxemia. It is of significance that we found that the effectiveness of pharmacological blockade of PKC, mitochondrial Bax translocation or Bax-associated mitochondrial apoptotic signaling against cardiovascular depression was dependent on the time of administration after LPS treatment. These novel observations pointed to the importance of therapeutic windows when targeting different cellular events in the design of management strategies against endotoxin-induced cardiovascular depression.

Downloaded from molpharm.aspetjournals.org at ASPET Journals on April 16, 2024

Acknowledgments

This work was carried out during the tenure of S.H.H.C. as the National Chair Professor of Neuroscience appointed by the Ministry of Education, and Sun Yat-sen Research Chair Professor appointed by the National Sun Yat-sen University, Taiwan, Republic of China.

Molecular Pharmacology Fast Forward. Published on January 16, 2007 as DOI: 10.1124/mol.106.031161
This article has not been copyedited and formatted. The final version may differ from this version.

References

Adams JM and Cory S (1998) The Bcl-2 protein family: arbiters of cell survival. *Science* 281:1322-1326.

Balafanova Z, Bolli R, Zhang J, Zheng Y, Pass JM, Bhatnagar A, Tang XL, Wang O, Cardwell E and Ping P (2002) Nitric oxide (NO) induces nitration of protein kinase Cε (PKCε), facilitating PKCε translocation via enhanced PKCε -RACK2 interactions: a novel mechanism of no-triggered activation of PKCε. *J Biol Chem* 277:15021-15027.

Bonfoco E, Krainc D, Ankarcrona M, Nicotera P and Lipton SA (1995) Apoptosis and necrosis: two distinct events induced, respectively, by mild and intense insults with *N*-methyl-D-aspartate or nitric oxide/superoxide in cortical cell cultures. *Proc Natl Acad Sci USA* 92:7162-7166.

Bright R and Mochly-Rosen D (2005) The role of protein kinase C in cerebral ischemic and reperfusion injury. *Stroke* 36:2781-2790.

Bright R, Raval AP, Dambner JM, Perez-Pinzon MA, Steinberg GK, Yernari MA and Mochly-Rosen D (2004) Protein kinase C δ mediates cerebral reperfusion injury in vivo. *J Neurosci* 24:6880-6888.

Buchner K, Adamec E, Beermann ML and Nixon RA (1999) Isoform-specific translocation of protein kinase C following glutamate administration in primary hippocampal neurons. *Mol Brain Res* 64:222-235.

Cao G, Minami M, Pei W, Yan C, Chen D, O'Horo C, Graham SH and Chen J (2001) Intracellular Bax translocation after transient cerebral ischemia: implication for a role of the mitochondrial apoptotic signaling pathway in ischemic neuronal death. *J Cereb Blood Flow Metab* 21:321-333.

Chan JYH, Wang SH and Chan SHH (2001a) Differential roles of iNOS and nNOS at rostral ventrolateral medulla during experimental endotoxemia in the rat. *Shock* 15:65-72.

Chan SHH, Wang LL, Ou CC and Chan JYH (2002) Contribution of peroxynitrite to

Downloaded from molpharm.aspetjournals.org at ASPET Journals on April 16, 2024

Molecular Pharmacology Fast Forward. Published on January 16, 2007 as DOI: 10.1124/mol.106.031161
This article has not been copyedited and formatted. The final version may differ from this version.

fatal cardiovascular depression induced by overproduction of nitric oxide in rostral ventrolateral medulla of the rat. *Neuropharmacology* 43:889-898.

Chan SHH, Wang LL, Wang SH and Chan JYH (2001b) Differential cardiovascular responses to blockade of nNOS or iNOS in rostral ventrolateral medulla of the rat. *Br J Pharmacol* 133:606-614.

Chan SHH, Wu KLY, Wang LL and Chan JYH (2005) Nitric oxide- and superoxide-dependent mitochondrial signaling in endotoxin-induced apoptosis in the rostral ventrolateral medulla of rats. *Free Radic Biol Med* 39:603-618.

Chang AYW, Chan JYH, Chou JLJ, Li FCH, Dai KY and Chan SHH (2006) Heat shock protein 60 in rostral ventrolateral medulla reduces cardiovascular fatality during endotoxemia in the rat. *J Physiol* 574:547-564.

Chuang YC, Tsai JL, Chang AYW, Chan JYH and Chan SHH (2002) Dysfunction of the mitochondrial respiratory chain in the rostral ventrolateral medulla during experimental endotoxemia in the rat. *J Biomed Sci* 9:542-548.

Comalada M, Xaus J, Valledor AF, Lopez-Lopez C, Pennington DJ and Celada A (2003) PKCε is involved in JNK activation that mediates LPS-induced TNF-α, which induces apoptosis in macrophages. *Am J Physiol Cell Physiol* 285:C1235-C1245.

Cooper GJ and Hunter M (1997) Intracellular pH and calcium in frog early distal tubule: effects of transport inhibitors. *J Physiol* 498:49-59.

Crisanti P, Leon A, Lim DM and Omri B (2005) Aspirin prevention of NMDA-induced neuronal death by direct protein kinase C zeta inhibition. *J Neurochem* 93:1587-1593.

Dickhout JG, Hossain GS, Pozza LM, Zhou J, Lhotak S and Austin RC (2005) Peroxynitrite causes endoplasmic reticulum stress and apoptosis in human vascular endothelium: implication in atherogenesis. *Arterioscler Thromb Vasc Biol* 25:2623-2629.

Eefting F, Rensing B, Wigman J, Pannekoek WJ, Liu WM, Cramer MJ, Lips DJ and Doevendans PA (2004) Role of apoptosis in reperfusion injury. *Cardiovasc Res*

Downloaded from molpharm.aspetjournals.org at ASPET Journals on April 16, 2024

Molecular Pharmacology Fast Forward. Published on January 16, 2007 as DOI: 10.1124/mol.106.031161
This article has not been copyedited and formatted. The final version may differ from this version.

61:414-426.

Halestrap AP and Brennerb C (2003) The adenine nucleotide translocase: a central component of the mitochondrial permeability transition pore and key player in cell death. *Curr Med Chem* 10:1507-1525.

Kantrow SP, Taylor DE, Carraway ME and Piantadosi CA (1997) Oxidative metabolism in rat hepatocytes and mitochondria during sepsis. *Arch Biochem Biophys* 345:278-288.

Kroemer G (1997) The proto-oncogene Bcl-2 and its role in regulating apoptosis. *Nat Med* 3:614-620.

Kuo TBJ, Yang CCH and Chan SHH (1997) Selective activation of vasomotor component of SAP spectrum by nucleus reticularis ventrolateralis in rats. *Am J Physiol* 272:H485-H492.

Li Y, Takemura G, Kosai K, Takahashi T, Okada H, Miyata S, Yuge K, Nagano S, Esaki M, Khai NC, Goto K, Mikami A, Maruyama R, Minatoguchi S, Fujiwara T and Fujiwara H (2004) Critical role for the Fas/Fas ligand system in postinfarction ventricular remodeling and heart failure. *Circ Res* 95:627-636.

Liu X, Kim CN, Yang J, Jemmerson R and Wang X (1996) Induction of apoptotic program in cell-free extracts: requirement for dATP and cytochrome *c*. *Cell* 86:147-157.

Lochner A, Marais E, Genade S and Moolman JA (2000) Nitric oxide: a trigger for classic preconditioning? *Am J Physiol Heart Circ Physiol* 279:H2752-H2765.

Martinou JC and Green DR (2001) Breaking the mitochondrial barrier. *Nat Rev Mol Cell Biol* 2:63-67.

Pierchala BA, Ahrens RC, Paden AJ and Johnson EM Jr (2004) Nerve growth factor promotes the survival of sympathetic neurons through the cooperative function of the protein kinase C and phosphotidylinositol 3-kinase pathways. *J Biol Chem* 279:27986-27993.

Ross CA, Ruggiero DA, Park DH, Joh TH, Sved AF, Fernandez-Pardal J, Saavedra JM and Reis DJ (1984) Tonic vasomotor control by the rostral ventrolateral

Downloaded from molpharm.aspetjournals.org at ASPET Journals on April 16, 2024

Molecular Pharmacology Fast Forward. Published on January 16, 2007 as DOI: 10.1124/mol.106.031161
This article has not been copyedited and formatted. The final version may differ from this version.

medulla: effect of electrical or chemical stimulation of the area containing C_1 adrenaline neurons on arterial pressure, heart rate, and plasma catecholamines and vasopressin. *J Neurosci* 4:474-494.

Roucou X and Martinou JC (2001) Conformational change of Bax: a question of life or death. *Cell Death Diff* 8:875-877.

Saito A, Narasimhan P, Hayashi T, Okuno S, Ferrand-Drake M and Chan PH (2004) Neuroprotective role of a proline-rich Akt substrate in apoptotic neuronal cell death after stroke: Relationship with nerve growth factor. *J Neurosci* 24:1584-1593.

Sharahar T, Gray F, Lorin de la Grandomaison G, Hopkinson NS, Ross E, Dorandeu A, Orlikowski D, Raphael JC, Gajdos P and Annane D (2003) Apoptosis of neurons in cardiovascular autonomic centers triggered by inducible nitric oxide synthase after death from septic shock. *Lancet* 362:1799-1805.

Shimizu S, Narita M and Tsujimoto Y (1999) Bcl-2 family proteins regulate the release of apoptogenic cytochrome *c* by the mitochondrial channel VDAC. *Nature* 399:483-487.

Siu PM and Always SE (2006) Deficiency of the Bax gene attenuates denervation-induced apoptosis. *Apoptosis* 11:967-981.

Takahashi A and Earnshaw WC (1996) ICE-related proteases in apoptosis. *Curr Opin Genet Dev* 6:50-55.

Wang X, Wang Y, Zhang J, Kum HP, Ryter SW and Choi AMK (2005) FLIP protects against hypoxia-reoxygenation-induced endothelial cell apoptosis by inhibiting Bax activation. *Mol Cell Biol* 25:4742-4751.

Weinreb O, Bar-Am O, Amit T, Chillag-Talmor O and Youdim MBH (2004) Neuroprotection via pro-survival protein kinase C isoforms associated with Bcl-2 family members. *FASEB J* 18:1471-1473.

Wolter KG, Hsu YT, Smith CL, Nechushtan A, Xi XG and Youle RJ (1997) Movement of Bax from the cytosol to mitochondria during apoptosis. *J Cell Biol* 139:1281-1292.

Downloaded from molpharm.aspetjournals.org at ASPET Journals on April 16, 2024

Molecular Pharmacology Fast Forward. Published on January 16, 2007 as DOI: 10.1124/mol.106.031161
This article has not been copyedited and formatted. The final version may differ from this version.

Wu KLH, Chan SHH, Chao YM and Chan JYH (2003) Expression of pro-inflammatory cytokine and caspase genes promotes neuronal apoptosis in pontine reticular formation after spinal cord transection. *Neurobiol Dis* 14:19-31.

Yang CH, Shyr MH, Kuo TBJ, Tan PPC and Chan SHH (1995) Effects of propofol on nociceptive response and power spectra of electroencephalographic and systemic arterial pressure signals in the rat: correlation with plasma concentration. *J Pharmacol Exp Ther* 275:1568-1574.

Yethon JA, Epand RF, Leber B, Epand RM and Andrews DW (2003) Interaction with a membrane surface triggers a reversible conformational change in Bax normally associated with induction of apoptosis. *J Biol Chem* 278:48935-48941.

Downloaded from molpharm.aspetjournals.org at ASPET Journals on April 16, 2024

Molecular Pharmacology Fast Forward. Published on January 16, 2007 as DOI: 10.1124/mol.106.031161
This article has not been copyedited and formatted. The final version may differ from this version.

Footnotes

This study was supported by research grants NSC-95-2752-B-075B-001-PAE (JYHC) and NSC-95-2752-B-110-001-PAE (SHHC) from the National Science Council, and VGHKS95-036 (JYHC) from Kaohsiung Veterans General Hospital, Taiwan, Republic of China.

Address Correspondence to: Dr. Samuel H.H. Chan, Center for Neuroscience, National Sun Yat-sen University, Kaohsiung 80424, Taiwan, Republic of China. E-mail: schan@mail.nsysu.edu.tw

Downloaded from molpharm.aspetjournals.org at ASPET Journals on April 16, 2024

Molecular Pharmacology Fast Forward. Published on January 16, 2007 as DOI: 10.1124/mol.106.031161
This article has not been copyedited and formatted. The final version may differ from this version.

Fig. 1. Representative immunoblots (insets) or densitometric analysis showing temporal changes in protein levels of PKC-α, PKC-βI, PKC-γ (A) or PKC-δ, PKC-ε or PKC-ζ (B) detected from membranous or cytosolic fraction of samples from ventrolateral medulla after intravenous administration of LPS (15 mg/kg). Values are mean ± SE of quadruplicate analyses on samples pooled from 5 to 6 animals in each group. *$p < 0.05$ versus sham-control (C) group in the Scheffé multiple-range analysis.

Fig. 2. Representative immunoblots (A) or densitometric analysis (B) showing temporal changes in protein levels of PKC-βI, PKC-γ or PKC-ζ detected from membranous fraction of samples from ventrolateral medulla in rats that received microinjection into the bilateral RVLM of aCSF or SMT (250 pmol) immediately after intravenous administration of LPS (15 mg/kg). Values are mean ± SE of quadruplicate analyses on samples pooled from 5 to 6 animals in each group. *$p < 0.05$ versus sham-control (C) group, and $^{\#}p < 0.05$ versus LPS group in the Scheffé multiple-range analysis.

Downloaded from molpharm.aspetjournals.org at ASPET Journals on April 16, 2024

Molecular Pharmacology Fast Forward. Published on January 16, 2007 as DOI: 10.1124/mol.106.031161
This article has not been copyedited and formatted. The final version may differ from this version.

Fig. 3. Representative results from immunoprecipitation (IP) followed by immunoblot (IB) assay on samples from ventrolateral medulla in rats that received microinjection into the bilateral RVLM of aCSF or SMT (250 pmol) (A,B), calphostin C (100 pmol) or Gö6983 (100 pmol) (C) or furosemide (D), immediately after intravenous administration of LPS (15 mg/kg). (A) and (B) illustrate temporal changes in expression of Bax or activated Bax (6A7) immunoprecipitated by anti-PKC, anti-Bax or anti-6A7 antiserum from cytosolic fraction. (C) and (D) show the level of Bax immunoprecipitated by anti-6A7 antiserum in total protein, or cytosolic or mitochondrial fraction 120 min after LPS administration. Mitochondrial heat shock protein 70 (Mt. HSP70) serves as a control for purity of the mitochondrial fraction and loading of protein. For clarity, results from 1% DMSO, the vehicle control for Gö6983, were not shown since they were similar to those of aCSF.

Fig. 4. (A). Representative results from immunoprecipitation (IP) followed by immunoblot (IB) assay showing temporal changes in expression of ANT, VDAC. Bcl-2 or Bcl-xL immunoprecipitated by anti-6A7 antiserum in mitochondrial fraction of samples from ventrolateral medulla in rats that received microinjection into the bilateral RVLM of aCSF or furosemide (10 nmol), immediately after intravenous administration of LPS (15 mg/kg). (B). Densitometric analysis of levels of ANT or VDAC immunoprecipitated by anti-6A7 antiserum from mitochondrial fraction 120 min after LPS administration and microinjection bilaterally into the RVLM of BCI (0.5 nmol) or BA (1 μmol). Values are mean ± SE of quadruplicate analyses on samples pooled from 5 to 6 animals in each group. $^{*}p < 0.05$ versus sham-control (C) group, and $^{\#}p < 0.05$ versus LPS group in the Scheffé multiple-range analysis.

Downloaded from molpharm.aspetjournals.org at ASPET Journals on April 16, 2024

Molecular Pharmacology Fast Forward. Published on January 16, 2007 as DOI: 10.1124/mol.106.031161
This article has not been copyedited and formatted. The final version may differ from this version.

Fig. 5. (A). Representative immunoblots showing temporal changes in cytochrome *c* detected from membranous or cytosolic fraction, or full-length or cleaved or caspase 3 from cytosolic fraction of samples from ventrolateral medulla in rats that received microinjection into the bilateral RVLM of aCSF or BCI (0.5 nmol) immediately after intravenous administration of LPS (15 mg/kg). (B). Quantitative analysis of temporal changes in DNA fragmentation in ventrolateral medulla of rats that received microinjection into the bilateral RVLM of aCSF, furosemide (10 nmol), BCI (0.5 nmol), BA (1 μmol) or Z-DEVD-fmk (100 nmol) immediately after LPS or saline administration. For clarity, results from 1% DMSO, the vehicle control for BCI and Z-DEVD-fmk, were not shown since they were similar to those of aCSF. Values are mean ± SE, n = 6-7 animals per group. $*p < 0.05$ versus sham-control (C) group, and $^{\#}p < 0.05$ versus LPS+aCSF group in the Scheffé multiple-range analysis.

Fig. 6. Temporal changes in MSAP, HR or power density of vasomotor components of SAP spectrum in rats that received intravenous administration of saline or LPS (15 mg/kg), given alone or with additional microinjection into the bilateral RVLM of aCSF or calphostin C, immediately (A) or 120 min (B) after the endotoxin. Values are mean ± SE, n = 6-7 animals per group. $*p < 0.05$ versus saline group, and $^{\#}p < 0.05$ versus LPS or LPS+aCSF group in the Scheffé multiple-range analysis. Arrows denote time during which microinjection was delivered.

Downloaded from molpharm.aspetjournals.org at ASPET Journals on April 16, 2024

Molecular Pharmacology Fast Forward. Published on January 16, 2007 as DOI: 10.1124/mol.106.031161
This article has not been copyedited and formatted. The final version may differ from this version.

Fig. 7. Temporal changes in MSAP, HR or power density of vasomotor components of SAP spectrum in rats that received intravenous administration of saline or LPS (15 mg/kg), given alone or with additional microinjection into the bilateral RVLM of 1% DMSO or BCI, immediately (A) or 120 min (B) after the endotoxin. Values are mean ± SE, n = 6-7 animals per group. *$p < 0.05$ versus saline group, and $^{\#}p < 0.05$ versus LPS or LPS+DMSO group in the Scheffé multiple-range analysis. Arrows denote time during which microinjection was delivered.

Fig. 8. Maximal changes in MSAP, HR or power density of vasomotor components of SAP spectrum in rats that received intravenous administration of saline (–) or LPS (15 mg/kg) with additional microinjection into the bilateral RVLM of aCSF, DMSO or calphostin C (100 pmol), furosemide (10 nmol), V5 (20 pmol), P5 (20 pmol), BCI (1 nmol), BA (10 nmol) or Z-DEVD-fmk (100 nmol), immediately (A) or 120 min (B) after the endotoxin. Values are mean ± SE, n = 6-8 animals per group. *$p < 0.05$ versus saline group, and $^{\#}p < 0.05$ versus LPS+aCSF or DMSO group in the Scheffé multiple-range analysis.

Downloaded from molpharm.aspetjournals.org at ASPET Journals on April 16, 2024

Molecular Pharmacology Fast Forward. Published on January 16, 2007 as DOI: 10.1124/mol.106.031161
This article has not been copyedited and formatted. The final version may differ from this version.

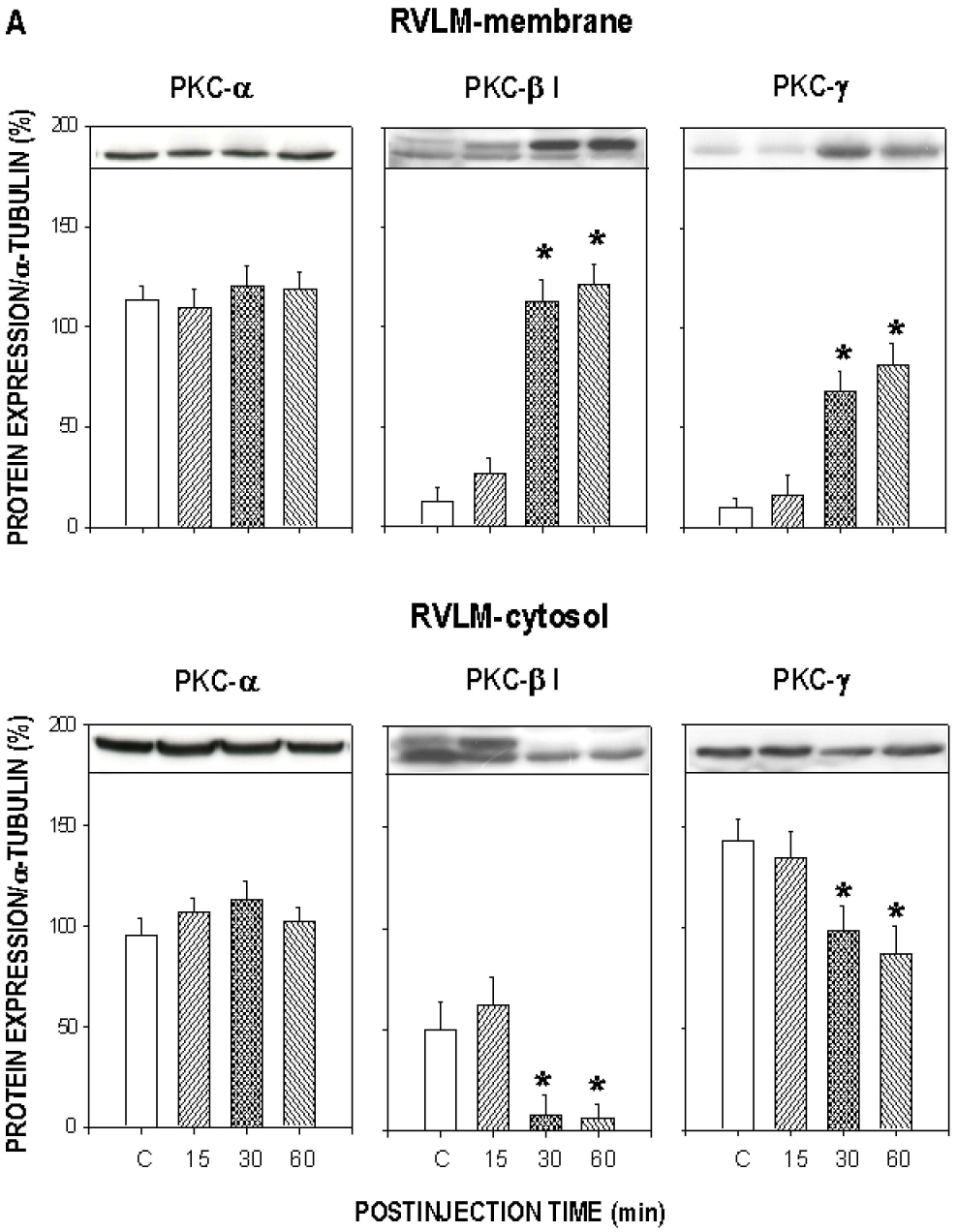

Figure 1 (part 1)

Molecular Pharmacology Fast Forward. Published on January 16, 2007 as DOI: 10.1124/mol.106.031161
This article has not been copyedited and formatted. The final version may differ from this version.

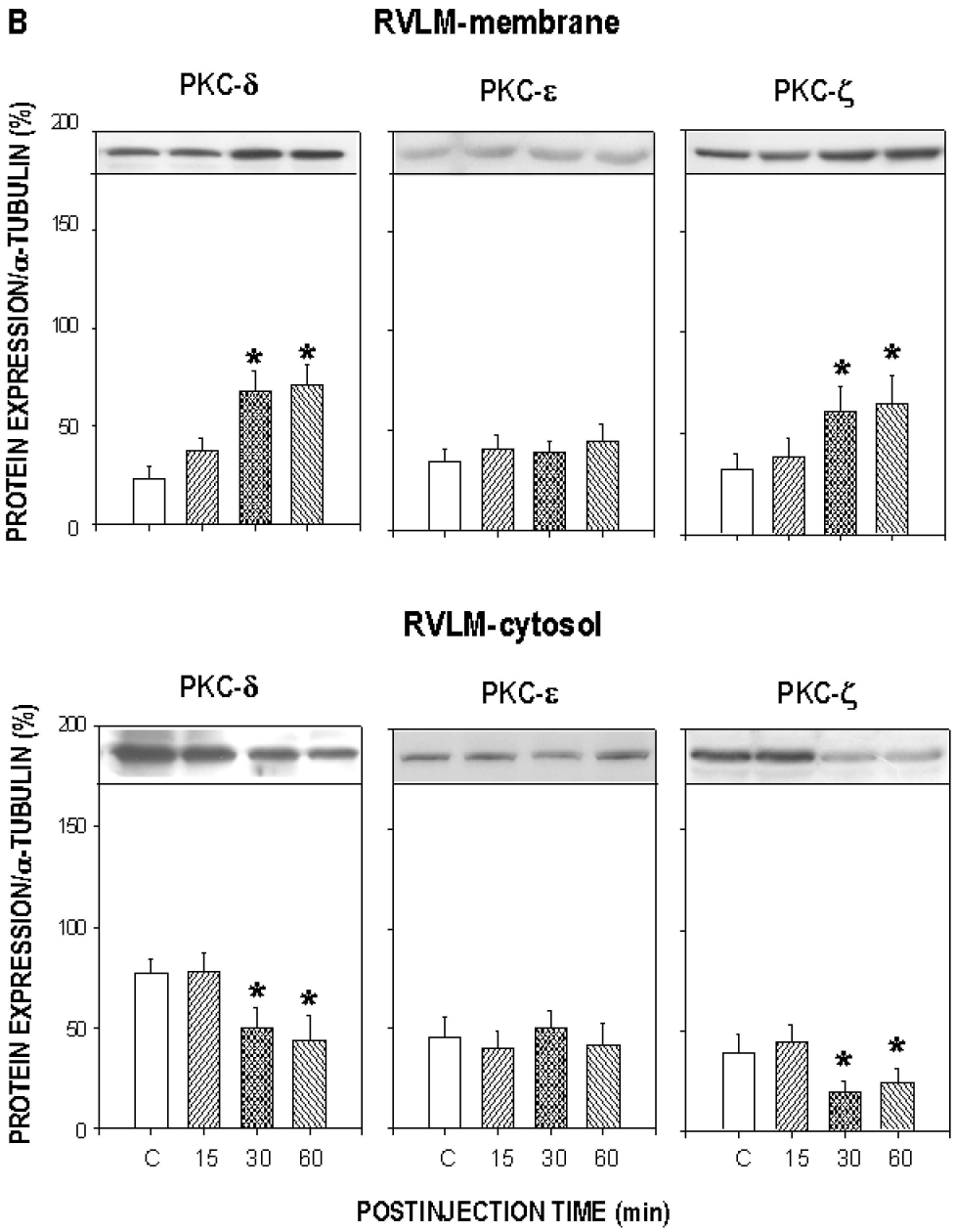

Figure 1 (part 2)

Molecular Pharmacology Fast Forward. Published on January 16, 2007 as DOI: 10.1124/mol.106.031161
This article has not been copyedited and formatted. The final version may differ from this version.

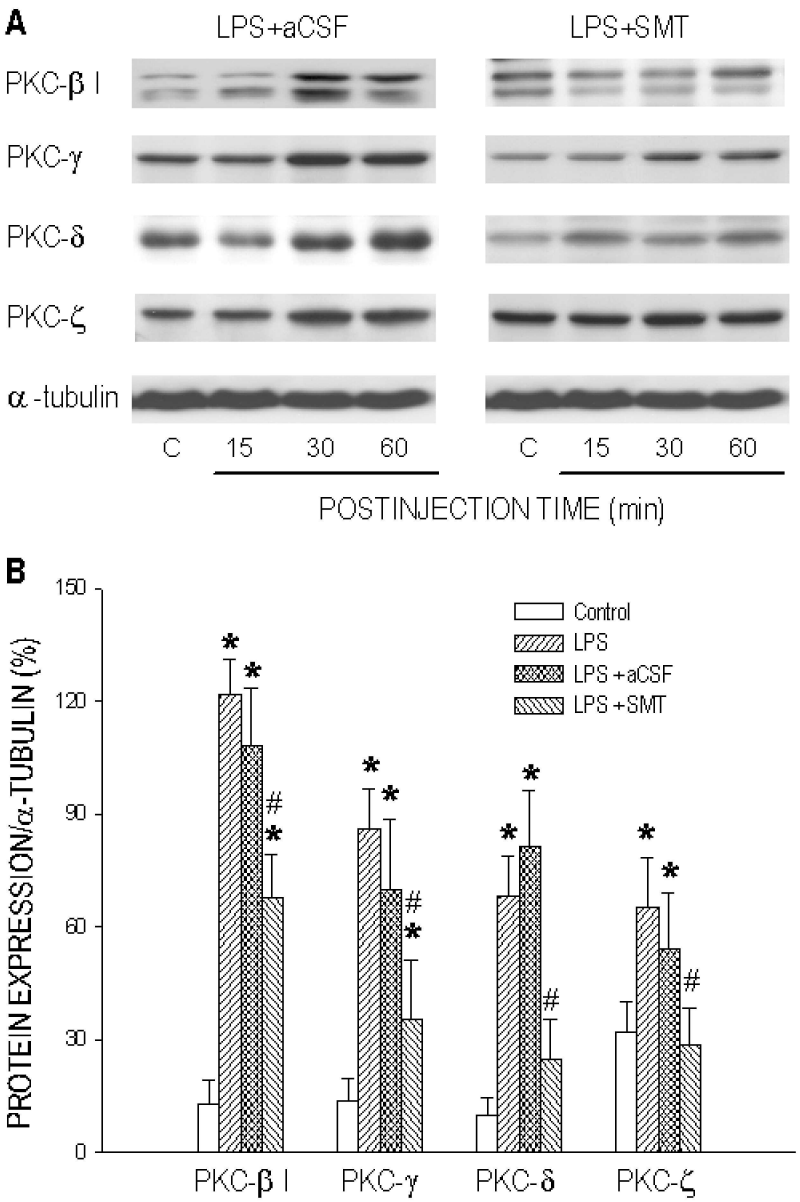

Figure 2

Molecular Pharmacology Fast Forward. Published on January 16, 2007 as DOI: 10.1124/mol.106.031161
This article has not been copyedited and formatted. The final version may differ from this version.

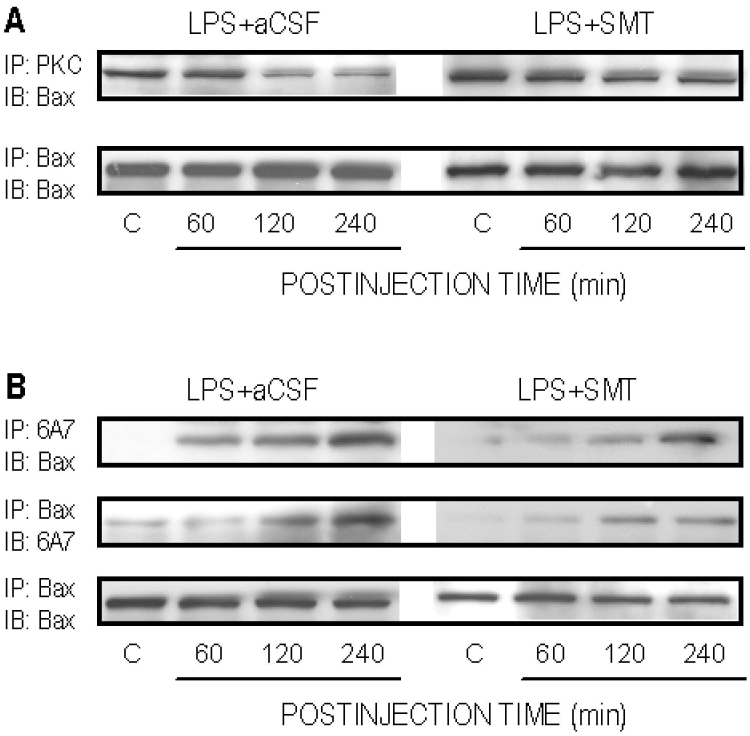

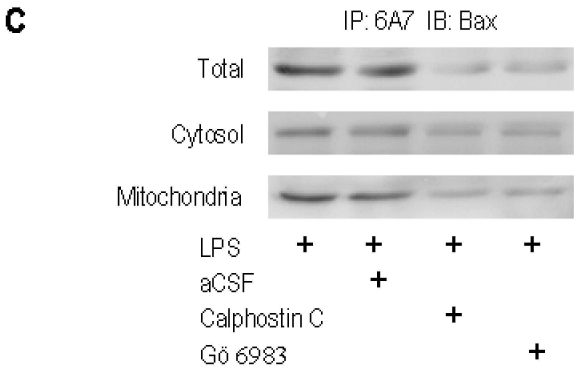

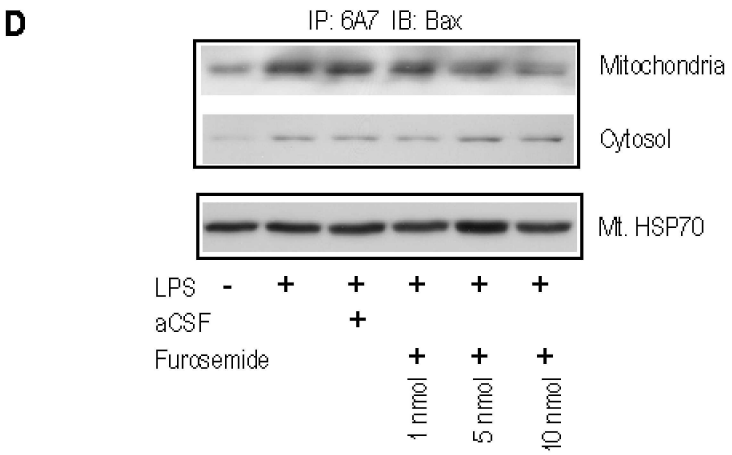

Figure 3

Molecular Pharmacology Fast Forward. Published on January 16, 2007 as DOI: 10.1124/mol.106.031161
This article has not been copyedited and formatted. The final version may differ from this version.

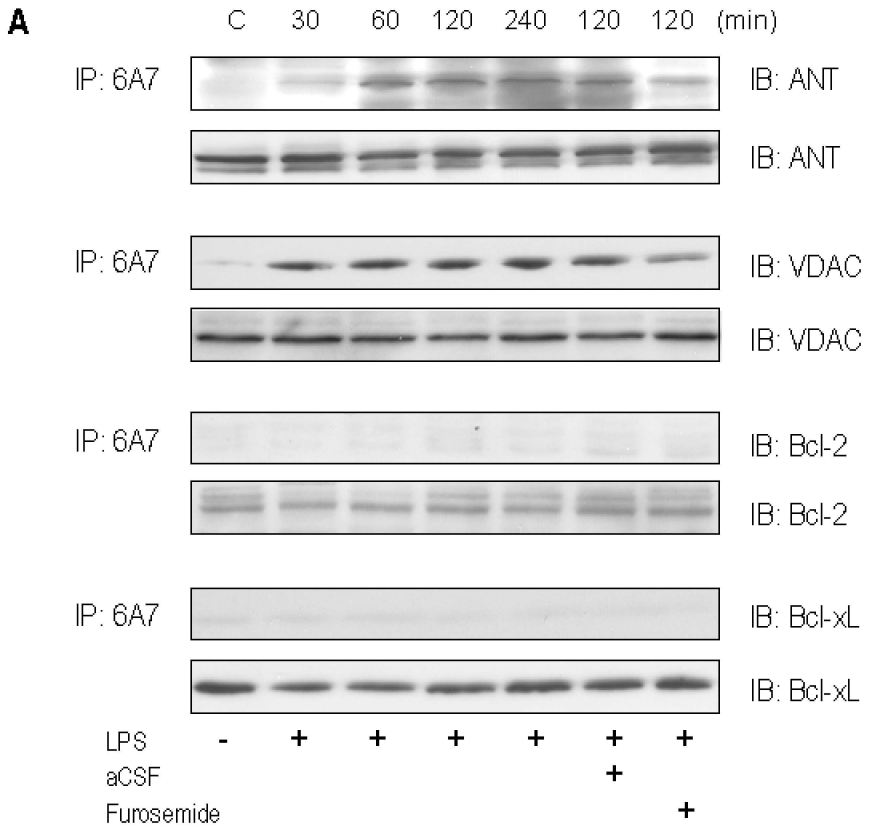

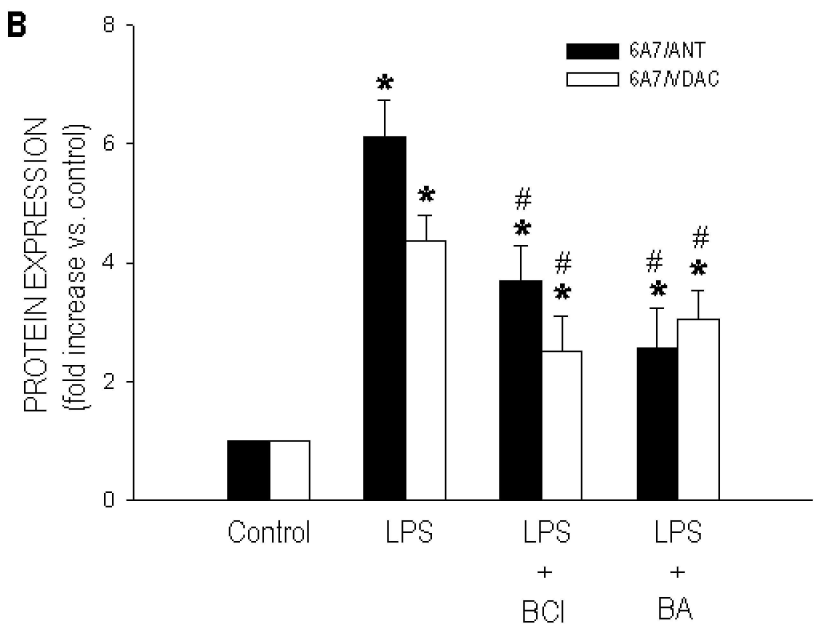

Figure 4

Molecular Pharmacology Fast Forward. Published on January 16, 2007 as DOI: 10.1124/mol.106.031161
This article has not been copyedited and formatted. The final version may differ from this version.

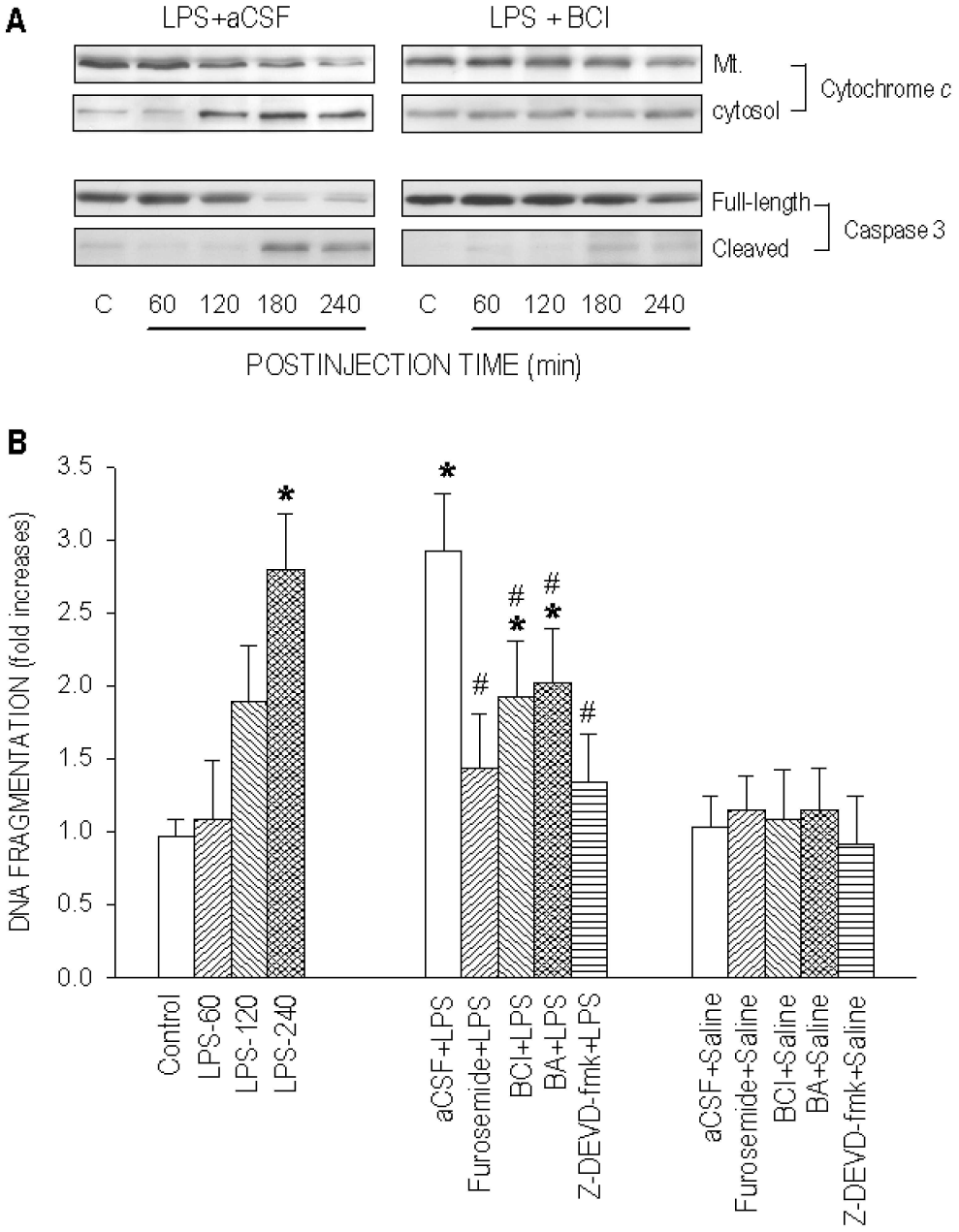

Figure 5

Molecular Pharmacology Fast Forward. Published on January 16, 2007 as DOI: 10.1124/mol.106.031161
This article has not been copyedited and formatted. The final version may differ from this version.

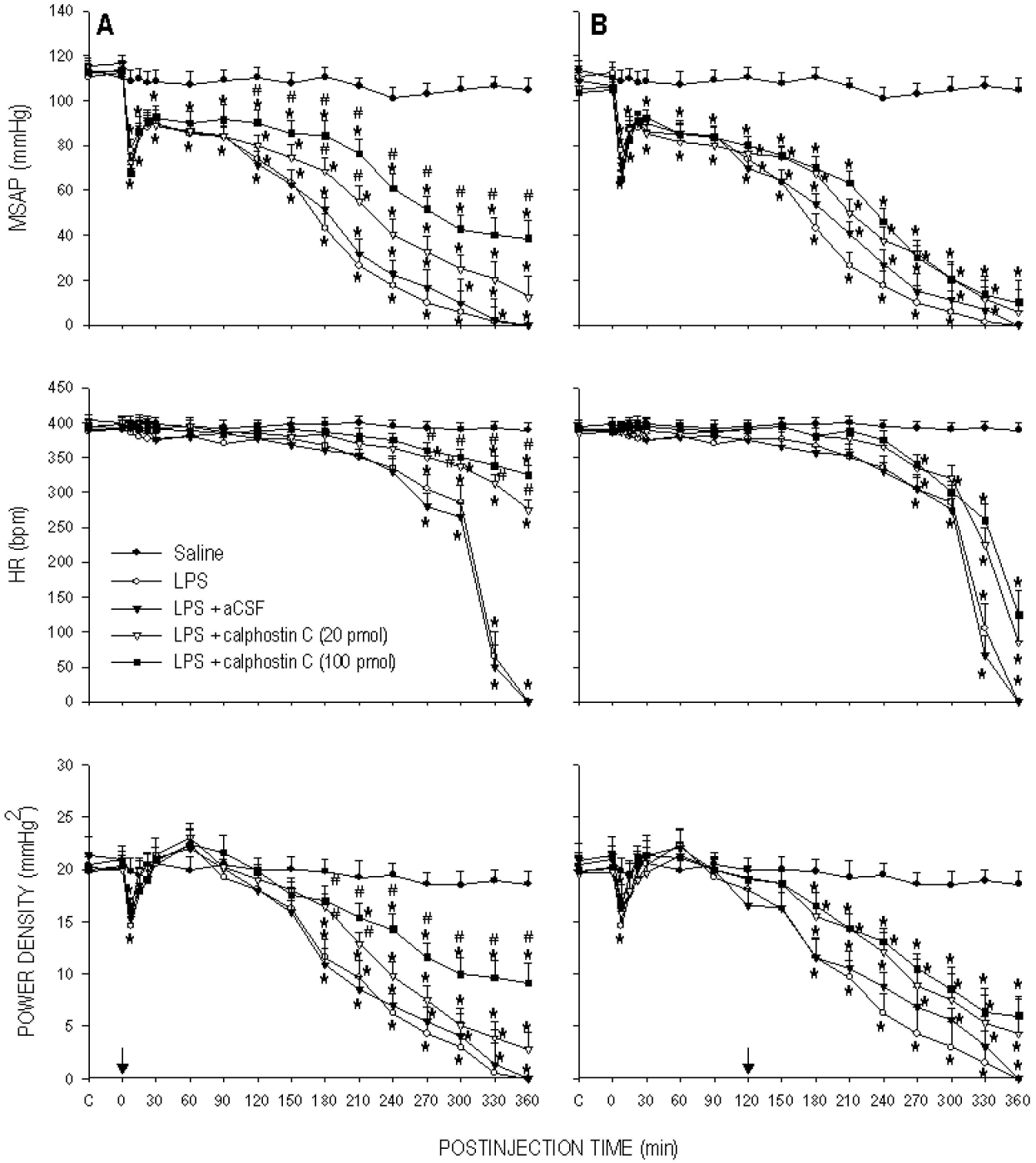

Figure 6

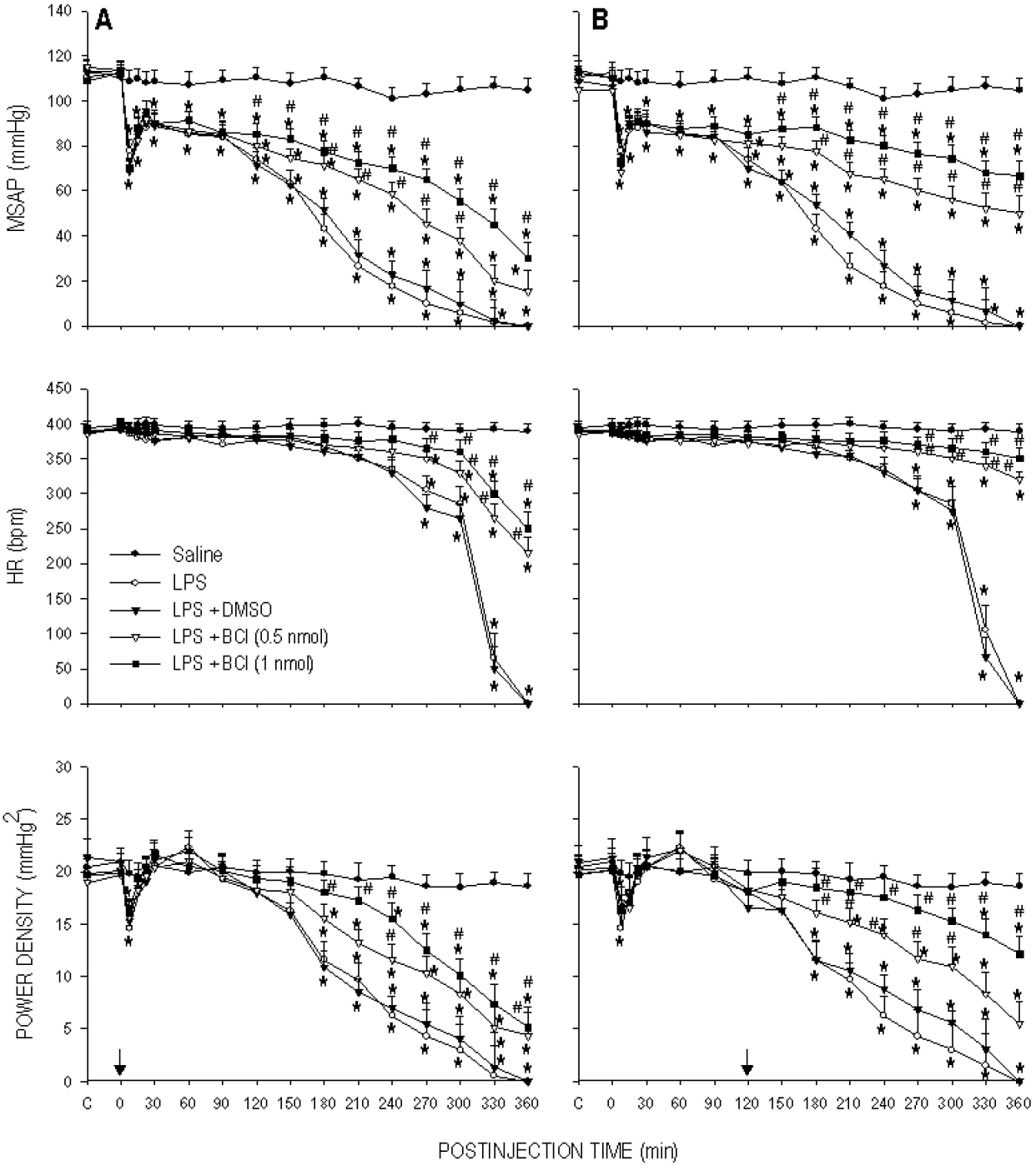
A
B
MSAP (mmHg)
HR (bpm)
POWER DENSITY (mmHg^2)
Saline
LPS
LPS +DMSO
LPS +BCl (0.5 nmol)
LPS +BCl (1 nmol)
C 0 30 60 90 120 150 180 210 240 270 300 330 360
POSTINJECTION TIME (min)

Figure7

Molecular Pharmacology Fast Forward. Published on January 16, 2007 as DOI: 10.1124/mol.106.031161
This article has not been copyedited and formatted. The final version may differ from this version.

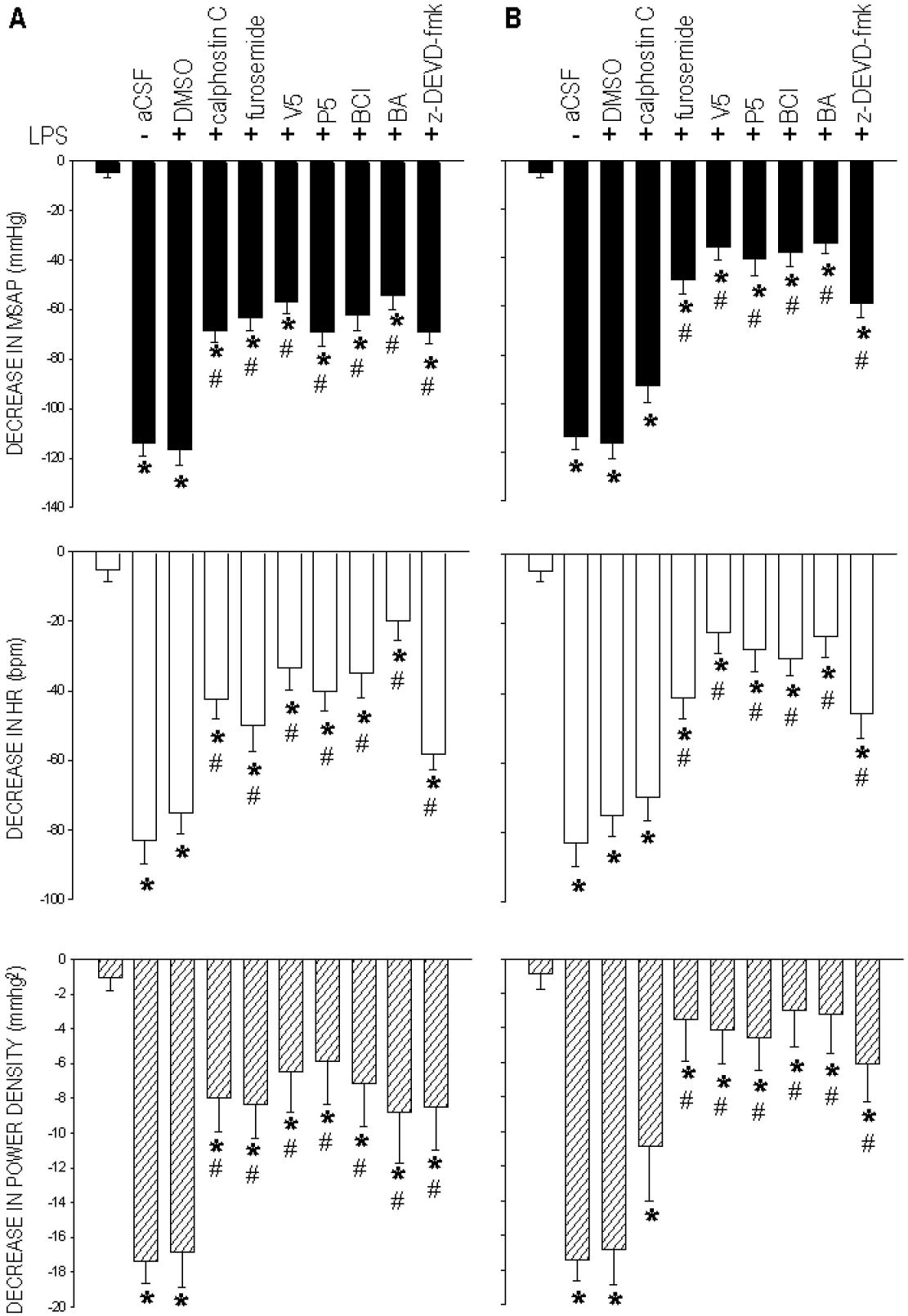

Figure 8